which is included in U_E, and the remainder (A10), which is the interaction via the screening electrons.

Probably the best available calculation of ϵ_1 as regards correlation and exchange is obtained, following Sham,[53–55] by applying Hubbard's[56] ansatz for the exchange terms, and using a screened interaction for the exchange. The result for ϵ_1 turns out to be

$$\frac{g^2\Omega}{8\pi e^2}\left[\frac{1}{\epsilon_1}-1\right]=\frac{f(g)}{\epsilon_2(g)}, \tag{A15}$$

where $\epsilon_2(g)$ is calculated[53,57] by the same ansatz. Substitution into (A10) gives again (A9), which is seen therefore to have a somewhat wider validity than was apparent in our simple derivation.

[53] L. J. Sham, thesis submitted to University of Cambridge, 1963 (unpublished); available on microfilm from Micro-methods Ltd., East Ardsley, Wakefield, England.
[54] L. J. Sham and J. M. Ziman, Solid State Phys. **15**, 221 (1963).
[55] L. J. Sham, Proc. Roy. Soc. (London) **A283**, 33 (1964).
[56] J. Hubbard, Proc. Roy. Soc. (London) **A276**, 308 (1964).
[57] Sham's ϵ_2 is given explicitly by V. Heine and I. Abarenkov, Phil. Mag. **9**, 451 (1964).

PHYSICAL REVIEW VOLUME 152, NUMBER 2 9 DECEMBER 1966

Electronic Specific Heat of Dilute Alloys: Fe(Ti), Fe(V), Fe(Cr), Fe(Mn), Fe(Co), Fe(Ni), Fe(Al), Fe(Si), Fe(Mo), Fe(W), and Ag(Au)

SAMUEL S. SHINOZAKI AND ANTHONY ARROTT
Scientific Laboratory, Ford Motor Company, Dearborn, Michigan
(Received 20 July 1966)

A method of measuring simultaneously the low-temperature specific heat of three samples, typically one pure-metal sample and two alloys with 1 and 2% solute, is described. The procedure is used to determine the variation of the electronic-specific-heat coefficient γ (the coefficient of the term linear in temperature) with concentration c for various solutes (Al, Si, Ti, V, Cr, Mn, Co, Ni, Mo, and W) in Fe and for Au in Ag. The simultaneous calorimetry gives an increase in relative accuracy sufficient to enable determination of variations of $(1/\gamma)d\gamma/dc$ to within $\pm 10\%$ for dilute alloys of Fe. For Ag(Au) alloys the variation of γ with concentration is less than can be detected in these experiments. A linear decrease of γ with increasing c is found for six of the iron-based alloy systems. For these the values of $(1/\gamma)d\gamma/dc$ are: Fe(Ti), -1.0; Fe(V), -2.2; Fe(Cr), -2.0; Fe(Mo), -0.8; Fe(W), -2.4; and Fe(Co), -0.6. A nonlinear increase of γ with c is found for the remaining. The average values of $(1/\gamma)d\gamma/dc$ are: Fe(Al), $+1.2$; Fe(Si), $+0.6$; Fe(Mn), $+2.0$; and Fe(Ni), $+2.6$. From experiments on two-phase alloys of Fe-Fe_2Nb, γ for Fe_2Nb is estimated to be between 9 and 10 mJ/deg^2 mole. There appears to be a correlation of $(1/\gamma)d\gamma/dc$ with certain aspects of Fe-alloy phase diagrams, namely, the variations of Curie temperature and the α-γ transformation temperature with concentration of solute.

I. INTRODUCTION

THE temperature dependence of the specific heat of a metal at low temperatures may be represented by

$$C=\gamma T+\beta T^3. \tag{1}$$

The term linear in temperature is the contribution to the specific heat from electronic excitations for temperatures low compared to the degeneracy temperature, $T_0=\epsilon_F/k$, where ϵ_F is the Fermi energy. The coefficient of this term is

$$\gamma=\pi^2k^2N(\epsilon_F)/3, \tag{2}$$

where $N(\epsilon_F)$ is the density of states of electronic energy at the Fermi energy. The second term represents the contributions from lattice vibrations. The coefficient β is given by

$$\beta=(12\pi/5)^4R/\Theta_D{}^3, \tag{3}$$

where R is the gas constant and Θ_D is the Debye temperature. This term adequately describes the lattice contribution only at temperatures very low compared to Θ_D. The temperature region experimentally accessible in liquid helium is usually sufficiently low. In this temperature region the two terms of Eq. (1) make comparable contributions to the specific heat and usually these account for almost all of it. Thus, it is standard practice to plot experimental data as C/T versus T^2, to fit a straight line to the data, and thus to obtain apparent values for γ and β. We denote these apparent values by γ^* and β^*.

We have measured the specific heat of Ag-based alloys and Fe-based alloys at temperatures between 2 and 4°K in order to obtain the variations of γ^* with concentration of solute for concentrations which may be considered dilute. We undertook this work in the hope of answering the question: Does γ^* have the same interpretations in a disordered alloy as in a periodic pure metal? This question was raised when Rayne[1] observed a rapid increase in γ^* of Cu(Zn) alloys. For a

[1] J. A. Rayne, Phys. Rev. **108**, 22 (1957).

sample with atomic fraction $c=0.03$ (3 at.%), he found $(1/\gamma^*)d\gamma^*/dc=2.3$. Yet the addition of Ni to Cu also increased γ^*. For a sample with $c=0.1$, Guthrie, Friedberg, and Goldman[2] had found $(1/\gamma^*)d\gamma^*/dc=5$. Such results do not follow from the rigid-band model,[3] which assumes that the same $N(\epsilon)$-versus-ϵ relation is applicable to a set of elements and alloys of a given crystal structure. The addition of Ni would decrease the number of electrons, whereas the addition of Zn would increase the number of electrons in the conduction band of Cu. If the rigid-band model were to apply, $d\gamma^*/d\bar{z}$ should be continuous through $\bar{z}=29$ for Cu. ($\bar{z}$ is the average atomic number of the alloy or the atomic number of the pure element.) But it is not. One might argue that there is actually an inverted cusp in the density-of-state curve at pure Cu, but this seems most improbable. The rigid-band model has its appeal in its simplicity. With it data can be analyzed to obtain band parameters. And specific-heat and magnetic-susceptibility or spontaneous-magnetization data may be fit to the same simple model.

The dilemma—how to keep a reasonable rigid-band model and explain the Cu(Zn)-Cu(Ni) results—might be resolved if the rigid-band model applied to sufficiently concentrated alloys but failed in some aspects for the dilute alloys. One might have conjectured that a shorter mean free path in the concentrated alloys was the key to this dilemma. Thus, it seemed desirable to test this conjecture by comparing γ^* of Cu with the γ^* of an alloy with the same z. This experiment was performed by Guthrie.[4] He prepared alloys of Cu with both Ni and Zn present in equal amounts, 3% of each in one alloy and 8% of each in another alloy. The values of γ^* for these "pseudo-copper" alloys showed that the increases from Ni and Zn were additive. Similarly motivated, Arrott and Skalyo[5] investigated a "pseudo-silver" alloy by adding to Ag a solute element of the same value and atomic size, namely Au. No change of γ^* outside the uncertainty of their measurements was found for alloys with $\frac{1}{2}$ and 1 at.% Au. As we had some doubt about the homogeneity of these samples, we have repeated that work using well-mixed, high-purity Ag alloyed with 1 and 2 at.% Au. Again, there is no change in γ^* outside experimental uncertainties. Green and Valladares[6] have recently measured higher concentration Ag(Au) alloys. They find a value of $(1/\gamma^*)d\gamma^*/dc=-0.3$. Our observations are not inconsistent with such a small rate of decrease. The relation of this result to other studies of γ^* for noble-metal alloys with group IIb, IIIb, and IVb alloys and to studies of the Fermi surface has been discussed at length by Green and Valladares. We present our observations on Ag(Au) alloys, obtained before the work of Green and Valladares, partially to confirm their findings, but mostly to establish the creditability of our other data by comparisons of our Ag(Au) data with their excellent work.

The situation in ferromagnetic iron is complicated because the Fermi surfaces of spin-up and spin-down electrons should not be the same. Further, it is not likely that only one of these surfaces contributes to the specific heat. Berger[7] has recently discussed the specific heat[8] and spontaneous magnetization[9] of Fe(Cr) and Fe(Co) alloys using rigid-band models. In this he explicitly says that the models do not account for that phenomena which is our main concern here, namely, a plot of γ^* versus $\bar{z}$ for Fe(Cr), Fe, and Fe(Co) shows a peak at pure Fe ($\bar{z}=26$) while as a whole the curve of γ^* versus $\bar{z}$ is falling rapidly from $\bar{z}=25$ onward. It is the over-all form of the curve of γ^* versus $\bar{z}$ which Berger considers and not the peak at Fe. The peak at Fe for the Fe(Cr)-Fe(Co) alloys is in contrast to the valley at Cu for the Cu(Ni)-Cu(Zn) alloys. This additional example of the deviation of a pure metal from the results of γ^* versus $\bar{z}$ for the alloys accounts partially for our desire to study the Fe-based alloys.

Mainly, however, we were attracted by the fact that from an experimentalist's viewpoint, Fe alloys are well suited to dilute-alloy studies. Some of the advantages, concerning metallurgical preparations, chemical analysis, and relatively large values for γ^* and spontaneous magnetizations, have been reviewed by Arrott and Noakes.[10] They have studied lattice parameters, spontaneous magnetization, Curie temperature, high-temperature susceptibility, and resistivity for a number of the same alloys for which we report observations of specific heat. These and/or similar alloys have also been investigated by means of the Mössbauer effect[11] and by small-angle neutron diffraction.[12] These latter two types of studies have given details on an atomic scale to consider along with the bulk physical properties in any

[2] G. L. Guthrie, S. A. Friedberg, and J. E. Goldman, Phys. Rev. **113**, 45 (1959).

[3] For a review of the rigid-band model as applied to the specific heat of alloys see F. E. Hoare, in *Electronic Structure and Alloy Chemistry of the Transition Elements*, edited by Paul A. Beck (Interscience Publishers, Inc., New York, 1963); N. F. Mott, Advan. Phys. **13**, 325 (1964).

[4] G. L. Guthrie, Phys. Rev. **113**, 793 (1959).

[5] A. Arrott and J. Skalyo (unpublished results), communicated briefly at the 1958 International Conference on the Electronic Properties of Metals at Low Temperatures, Geneva, New York (unpublished). Some experimental aspects of this work are mentioned in Sec. II.

[6] B. A. Green, Jr., and A. A. Valladares, Phys. Rev. **142**, 379 (1966).

[7] L. Berger, Phys. Rev. **137**, A220 (1965).

[8] C. H. Cheng, C. T. Wei, and P. A. Beck, Phys. Rev. **120**, 426 (1960); see also later work: E. A. Starke, Jr., C. H. Cheng, and P. A. Beck, *ibid.* **126**, 1746 (1962); K. P. Gupta, C. H. Cheng, and P. A. Beck, J. Phys. Chem. Solids **25**, 1147 (1964); C. H. Cheng, K. P. Gupta, C. T. Wei, and P. A. Beck, *ibid.* **25**, 759 (1964); N. Pessall, K. P. Gupta, C. H. Cheng, and P. A. Beck, *ibid.* **25**, 993 (1964).

[9] R. M. Bozorth, *Ferromagnetism* (B. Van Nostrand Company, Princeton, New Jersey, 1951).

[10] A. Arrott and J. E. Noakes, *Iron and Its Dilute Solid Solutions* (Interscience Publishers, Inc., New York, 1963), pp. 81–117; J. E. Noakes and A. Arrott, J. Appl. Phys. **37**, 1264 (1966), and (to be published).

[11] M. B. Stearns, Phys. Rev. **147**, 439 (1966), and Refs. 1–3 cited therein.

[12] M. F. Collins and G. G. Low, Proc. Phys. Soc. (London) **86**, 535 (1965).

theoretical treatment of the dilute alloys of Fe. Our work on specific heat is presented as a contribution to the increasing volume of experimental data on Fe and its dilute alloys.

We have studied dilute alloys of Fe with the other elements of the 1st transition series as solutes. Also we have measured γ^* for Fe with the solutes W and Mo, which together with Cr represent variation down a column in the periodic table. Finally, Al and Si were added to Fe to obtain some results representative of nontransition-metal solutes. The solute concentrations are of the order of 1 and 2 at.%. We cannot anticipate that these concentrations are necessarily sufficiently low to justify the use of the term dilute. We call them dilute because this is as low a range of concentration as our experimental techniques enable us to investigate. We will consider the results as representative of dilute alloys if we obtain a linear dependence of γ^* with concentration.

II. EXPERIMENTAL PRINCIPLES

The changes in γ which we encounter in this work are of the order of 1%. This was about the limit of accuracy of measurements undertaken up to the start of this investigation. We have employed a system of three-sample simultaneous calorimetry. As is conventional, we determine the heat input to a sample from measurements of the I^2R loss for a fixed time and calculate a temperature change from measurement of the resistance of a carbon resistor. Both these operations can be carried out with more accuracy than is usually reflected in the final specific-heat measurements. The difficulties arise in calibration of the carbon thermometers and in determining the contributions from the extra sources of heating. In the three-sample method these difficulties are diminished through cancellations of similar errors.

When this work was started the conventional measurement techniques used helium exchange gas as a "heat switch." Since then many other workers, like ourselves, have abandoned the exchange-gas technique in favor of mechanical heat switches following the work of Berman[13] on the conductivity of metal-to-metal contacts at helium temperatures. Also, it was the practice to calibrate thermometers by measuring the vapor pressure of a "pumped-on" helium bath surrounding the calorimetric can. We have adopted the technique of Hoare and Yates[14] wherein the carbon-resistance thermometers are calibrated directly in a helium-vapor bulb.

Before adoption of mechanical heat switches much effort was expended in attempts to obtain accurate results with helium gas as the heat switch. The difficulty is that adsorped helium, which is not removed by pumping, desorps on subsequent heating of the sample.

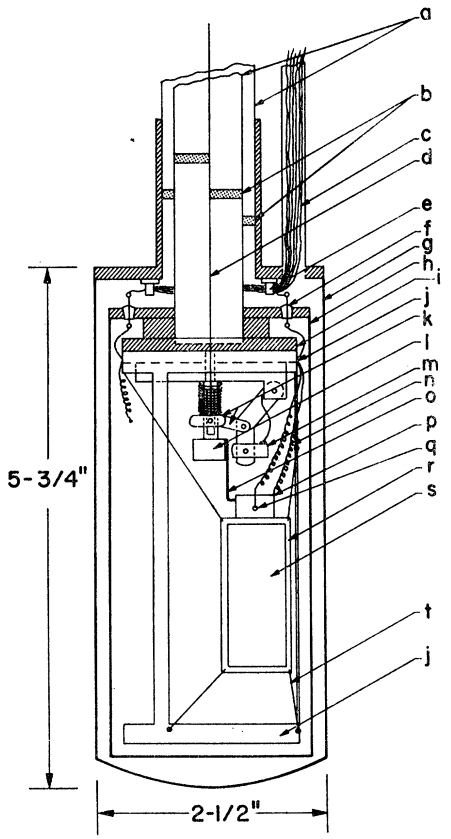

FIG. 1. The two concentric calorimeter cans (g and h) are shown in cutaway view while the support frame (j), part of the heat switch (d, k, l, m, and o), and one sample holder (r) are shown in direct view. Further notations are discussed in the text.

This may be detected by a change in the thermal conductance between the sample and the rest of the calorimeter. The thermal conductance is calculated from measurements of the drift rate between sample heating intervals and the knowledge of the heat capacity as determined in the experiment. We found a strong correlation between "bad" specific-heat points and those for which there was a change in conductance from before to after the heating interval. In other words, we used as a criterion for good data the applicability of Newton's law of cooling to the sequence of drift periods between the heating periods. Even after we adopted the mechanical heat switches we continued to apply Newton's law of cooling, since it serves as a check on the problem of heating from mechanical vibrations. As mechanical vibrations, particularly those of a transient nature, are generally much less severe at night; that is when our experiments are carried out. In addition, we attempt to tune the suspensions of our three samples to the same natural frequencies. This we have checked by observations of changes of the rates of heating with the frequency of a mechanical oscillator set on the bench which supports the cryostat.

The increased precision of the three-sample technique

[13] R. Berman, J. Appl. Phys. **27**, 318 (1956); see also discussion by G. K. White, *Experimental Techniques in Low Temperature Physics* (Clarendon Press, Oxford, England, 1959), p. 198.

[14] F. E. Hoare and B. Yates, Proc. Roy. Soc. (London) **240A**, 42 (1957).

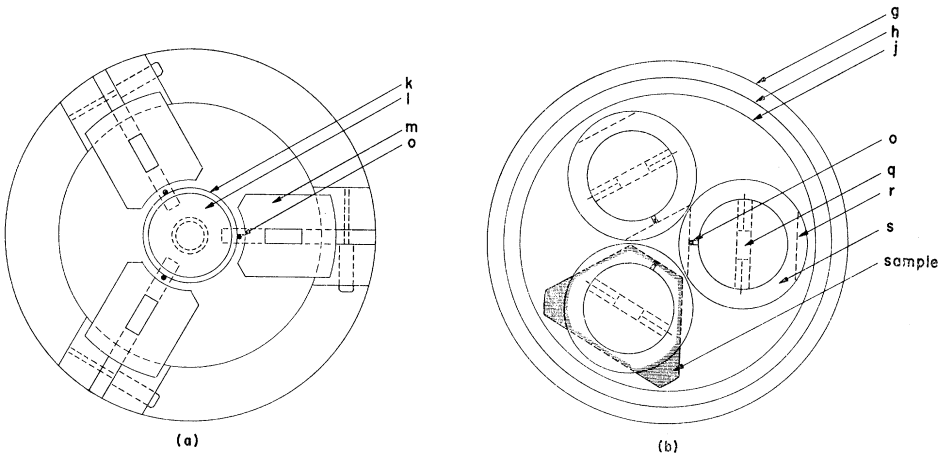

FIG. 2. (a) Top view of triple-jaw-action mechanical heat switch. (See text.) (b) Top view of three sample holders, one with sample in place. (See text.)

arises primarily from cancellation of systematic errors in thermometry. All three thermometers are calibrated together at the same set of temperatures. In all but our latest work we had noticeable systematic errors in the measurement of pressure. While these affect the absolute values of specific heat for any one sample, the effect on the differences between the samples is negligible. We calibrate the carbon resistance thermometers directly in the vapor above a helium liquid-vapor interface. During calibrations the helium bath surrounding the cryostat is held at a higher temperature than the isolated inner can which contains the helium liquid-vapor interface and the carbon thermometers. In this way the interface is always the coldest place to which the vapor has access. The vapor is slowly pumped in order to maintain the lower temperature. This procedure should eliminate errors which in other techniques may be traced to gradients between the liquid-vapor interface and the thermometers. In order to avoid problems with absorbed gas in the measurement of specific heat, the calibration is carried out after the specific-heat measurement.

The details of the calorimeter and of the measuring procedures are given in Sec. III. The main features of the calorimetry are a symmetric arrangement of three sample holders with attached heaters and thermometers, a three-jawed symmetric mechanical heat switch, the use of the inner copper calorimeter can as a vapor-pressure thermometer, the simultaneous measurements of the heat content for the three samples, and the simultaneous calibration of the three carbon-resistance thermometers.

III. EXPERIMENTAL APPARATUS AND TECHNIQUES

Figure 1 shows the concentric calorimetric cans (g and h) in a cutaway view from the side while the support frame (j), part of the heat switch (d, k, l, m, and o), and one sample holder (r) are shown as viewed directly from the side. The heat switch and three sample holders are symmetrically arranged as shown in the top views of Fig. 2. (Part of the heat switch and two of the sample holders are left out of Fig. 1 for clarity.) There are two concentric "down tubes" (a) to maintain the separate vacuums in the two calorimetric cans (g and h). These down tubes contain copper inserts (b) in a staggered array to block radiation from room temperature. A third down tube conducts the electrical lead wires (c) into the low-temperature region. The leads leave the vacuum region at room temperature through Kovar lead-through seals. The leads are thermally shunted to the helium bath by cementing them to copper posts (e) with G.E.-7031 adhesive and insulation varnish. Kovar seals (f) are used to bring the leads into the inner can. From an oil bath at ambient, through the Kovar seals at ambient, and to the top of the Kovar seals on the top of the inner can, the lead wires are No. 36 manganin. Inside the inner can, we use 0.002-in.-diam niobium (superconducting) leads which are helically wound to form a coil about $\frac{1}{2}$ in. long from 20 in. of wire. The ends of the niobium wires are copper-plated to permit solder connections.

The Heat Switch

Figures 1 and 2 show the mechanical heat switch with its three movable jaws (m) and a stationary center post (1) which can clamp the No. 24 copper wires (o) which are attached to each of the sample holders. The jaws close when a No. 3 piano wire (d) is put under tension, raising the ring (k). The ring (k) has a cross member to which the piano wire is attached centrally. The ring moves about $\frac{1}{8}$ in. to close the jaws on the copper wires. The spacing between (l) and (m) is $\frac{1}{16}$ in. Braided copper straps keep the movable jaws in thermal contact with the top of the inner can. On release of the tension in the piano wire a spring lowers the ring and opens the jaws. A bellows at the top of the inner down tube transmits force to the piano wire.

The high symmetry of the heat switch is desirable because the heating rate for some time after opening the

heat switch is determined by the vibrations imparted to the samples on release and it is important to keep the samples together in temperature for accurate comparison of specific heat among the three samples.

Sample Holders

The three sample holders (25 g of high-purity copper) are suspended by cotton threads (t) from a brass support frame (j). When the support frame is removed from the calorimeter, for ease in changing samples, neither the suspension threads nor the niobium lead wires are disturbed. The niobium leads join to short copper leads which are fixed to (but insulated from) the support frame. The other ends of the copper leads are soldered and unsoldered from the bottom of the Kovar seals on replacing and removing the support frame with its attached sample holders. Each holder is supported by seven cotton threads under tension. Cotton has the useful property of shrinking after being wetted and this serves to produce suitable tensions. As the samples are very close to one another and to the support frame the tension is necessary to prevent touching on vibration. The threads are arranged so as not to touch each other nor to block access to the sample mounting spaces (s).

One of the three sample holders is shown in profile in Fig. 1. The cylindrical head accommodates a carbon resistor, a manganin heater wire, and a copper wire which leads to the jaws of the heat switch. The resistors are 47-Ω, 0.1-W, Allen-Bradley carbon resistors selected by intercomparison of 50 resistors to find three with the most similar characteristics. The resistors are insulated by thin cigarette paper and glued into a small hole (q) running through the cylindrical head [see top view in Fig. 2(b)]. The heaters (p) are 500 Ω of No. 42 manganin wire with double formvar insulation wound around the circumference of the cylindrical head of the sample holder. Again we use a thin insulating layer of cigarette paper. We are careful to insure that the solder joints between the niobium leads and the manganin heater are well glued down. We found that, if thermal contact were not maintained, the specific-heat results would depend upon heater current. We suspect that the ends of the niobium leads do not remain superconducting during the heating periods if the ends of the manganin leads cannot dissipate heat radially. The No. 24 copper wire to the thermal switch is press fitted to the sample holder and secured with a 2–56 set screw.

The lower part of the sample holder has a large slot ($\frac{9}{16}$ in. wide and $1\frac{1}{4}$ in. high) which accommodates 60 g of iron sample when the samples are cut as shown in Fig. 2(b). The sides of the slot are parallel and highly polished. The surfaces of the sample are likewise parallel and highly polished. A slip fit is obtained, then a small amount of glycerin (volume determined by hypodermic syringe) is applied to the surfaces. The glycerin is used to maintain good thermal contact between the holders and the specimens, but also it lubricates and thus makes it easy to insert the samples without disturbing the suspension of the sample holders.

The vapor pressure of helium condensed in the calorimeter can is measured continuously during the calibration of the carbon resistance thermometers. In the earlier experiments we used a well and cistern-type mercury manometer (Exactel Servomanometer) and in the later experiments we used both the Exactel Servomanometer and a fused-quartz pressure gage (Texas Instruments).

The resistance measurements are made by the standard four-terminal technique with a Tinseley Vernier potentiometer and a Leeds and Northrup dc microvoltmeter. The Tinseley is used as a voltage suppression and the imbalance amplified by the dc microvoltmeter and recorded on a high pen speed, 10-mV, Weston strip chart recorder with paper speed of 15 sec per in. The precision of this combination is $\pm 0.1\ \mu$V. The Tinseley vernier potentiometer is well suited to this work as it has four sets of input terminals with a low-thermal-emf switch to rapidly select inputs. The three resistance thermometers are connected to a common ground (the only ground). Thus, three separate current supplies are used for the three resistance thermometers. The current supplies use Dynage Inc. 3-V (25-mA max) "Bat Sub" constant-voltage sources.

The current (3.0 μA) is allowed to vary slightly as the resistance of the thermometer changes with temperature. There is no error in this in that the calibration procedure is also done at constant voltage (at the source) rather than constant current.

The heaters are all connected in series. Current is drawn from the heater supply at all times either into the heater windings or into a dummy heater of the same resistance. This current is monitored continuously.

The heating periods are timed with a Hewlett-Packard electronic timer which is started and stopped by the making and breaking of the contacts of a Leeds and Northrup copper knife switch. This switch is mechanically tied to an identical switch which makes and breaks the connections to the heaters.

After the specific-heat measurements are completed the thermometers are calibrated. The first step is to liquify helium in the inner can. Between the can and a helium-gas cylinder, we connect the bladder of a soccer ball. We fill the bladder and then condense helium until 5 bladders full of gas are gone, that is about 40 cc of liquid helium are condensed. The helium in the Dewar surrounding the calorimeter is warmed to 4.2°K and the outer calorimeter can is evacuated. After some time we start to pump slowly on the helium in the inner can. We have an instantaneous response of the thermometers to the changes in vapor pressure. Part of the copper sample holder is under the surface of the helium and the calorimeter can itself is copper. There is no need to make corrections for hydrostatic head as the thermometers are in the vapor and the whole can is very close to an isothermal condition. There is no observable dis-

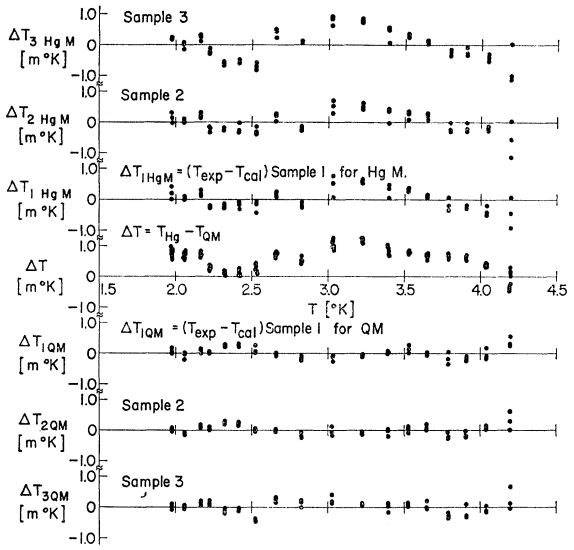

FIG. 3. The central graph compares the temperatures calculated from the mercury manometer and the quartz manometer. The upper three graphs show the fits to Eq. (1) for the three resistance thermometers in one experiment when the mercury manometer was used. The lower three graphs show the same thing for the quartz manometer.

continuity (less than 0.0001°K) in the curve of the temperature as determined from vapor-pressure measurements for continuous measurements through the λ point, where the properties of liquid helium change so drastically.

IV. TREATMENT OF DATA

The resistance-temperature relations are found using the 1958 international table for vapor pressure and temperature and the following empirical formula:

$$[\ln(R/R_0)/T]^{1/2}=A+B\ln(R/R_1)+C[\ln(R/R_0)]^2. \quad (4)$$

Heat capacities are calculated from

$$C=i^2R\Delta t/\Delta T, \quad (5)$$

where i is the heater current, R is the heater resistance, Δt is the heating time, and ΔT is the temperature change. The heat capacities are corrected for the heat capacities of the sample holders, converted to heat capacities per mole and fitted to the equation

$$C=\gamma T+\beta T^3. \quad (6)$$

These procedures are discussed below.

Thermometry

Though Eq. (4) contains four parameters, the choice of R_0 does not strongly affect the fit of the data. It has been customary for this equation to be used with $R_0=1\ \Omega$, but we find that $R_0=8\ \Omega$ gives an improved fit. With this value of R_0 we find A, B, and C by the method of least squares.

The fits to Eq. (4) are better for the fused-quartz pressure gage than for the mercury sevo-manometer. For the quartz gage the deviations from Eq. (4) are less than 0.0005°K. Over most of the range the fits are to ±0.0002°K. Comparison of the two pressure measuring devices shows a systematic deviation of the mercury servo-manometer which reaches a maximum of 0.4 mm in the middle of the range. The maximum apparent temperature difference calculated from the two pressure devices is 0.001°K. Figure 3 compares the temperatures calculated from the manometers and shows the fits to Eq. (4) for each of three carbon resistance thermometers for both manometers. There are three measurements at each temperature for each thermometer. If the coefficient of electronic specific heat γ is calculated using each set of pressure readings, the results for each sample differ by about 0.1%. Yet when one compares differences in γ between samples in a given run, the choice of manometer makes a difference of less than 0.01%. A more important difficulty was uncovered when the two manometers were first used together, namely that the zero of the mercury manometer had not been checked often enough and apparently had varied between runs. The maximum zero error has no effect (less than 0.01%) on the comparison of γ's for samples in a given run, but is the major contributor to the differences in absolute values found for the values of γ for iron in the earlier runs with only the mercury manometer, that is, those of alloys with Mn, Cr, V, Ti, Mo, W, and Nb. Thus, the later measurements using the two manometers we believe to give closer to the correct absolute values for Fe.

Though there are slight systematic deviations of the data from Eq. (4), we have not made further refinement in the curve fitting. Instead we rely on the fact that the fits of all three thermometers to Eq. (4) have the same systematic errors and that the measurements on the three samples are always between almost the same initial and final temperatures. Furthermore, we have demonstrated that the specific-heat differences between the three samples in any one run are not at all sensitive to such systematic errors.

Specific-Heat Coefficients

The temperature change ΔT upon heating to be used in Eq. (5) is determined by the standard procedure of extrapolation of temperature-versus-time curves from before and after a heating period into the middle of the heating period. This corrects for the extraneous heat lost or gained by the sample during the finite heating time. This procedure is appropriate if Newton's law of cooling is obeyed on both sides of the heating period. From the resistance (rather than temperatures) extrapolated to the center of the heating periods we calculate the temperature rise and the mean temperature. Together with the energy-input data these quantities then determine the specific heat as a function of temperature. The extraneous power into the samples

TABLE I. Comparison of results for silver.

	γ(mJ/°K^{-2} mole^{-1})	Θ_D(°K)
This work	0.656	225.3
Dixon *et al.*[a]	0.650	226.4
Filby and Martin[b]	0.646	226.2
Green and Culbert[c]	0.646	225.5
Green and Valladares[d]	0.654	225.8
Corak *et al.*[e]	0.637[f]	226.5[f]

[a] See Ref. 16.
[b] See Ref. 17.
[c] See Ref. 15.
[d] See Ref. 6.
[e] See Ref. 18.
[f] Corrected by J. Skalyo and A. Arrott (unpublished) for 1958 temperature-scale change and after removal of several bad points.

during the drift periods is also calculated. Thus, we determine that Newton's law of cooling is obeyed. It is a practical advantage of the three sample system that numerical errors are easily spotted and that the source of actual inaccuracies is readily traced. The three sample holders have heat capacities within 1% of each other over the entire temperature range and fit well to an expression for the heat capacity of the form of Eq. (6). The contribution of the sample holder to the total heat capacity is between 10 and 15% for Fe and its alloys and between 30 and 35% for Ag and its alloys. The contribution of the sample holders to any error in determining the differences in specific heat of Fe and its alloys is probably less than 0.1% of the total specific heat.

The many measurements reported here were made over an extended period of time during which the apparatus was modified from time to time. Our first measurements on Fe alloys (Group I), which included

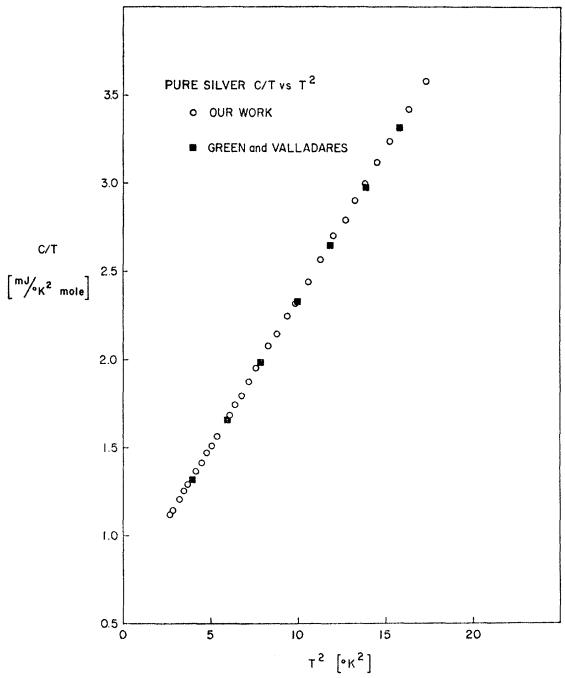

FIG. 4. Specific heat of silver shown on conventional C/T-versus-T^2 plot.

Fe(Mn), Fe(Cr), Fe(V), and Fe(Ti), were carried out to investigate the effects of "nonmagnetic" solutes of the first transition series on the specific heat of Fe. The second series (Group II) which included Fe(Mo), Fe(W), and Fe(Nb) was to investigate the effect of "nonmagnetic" solutes of the second and third transition series.

TABLE II. Results for iron and iron alloys.

$$C=\gamma T+\beta T^3\ [\text{mJ/°K mole}],\quad \Theta_D=\left(\frac{1943}{\beta}\right)^{1/3}\ [\text{°K}]$$

Experimental name	Group	Iron results γ	β	Θ_D	1st Alloys Atomic percent	$\Delta\gamma_1(a)$	$\Delta\beta_1(a)$	$\Delta\gamma_1(b)$	2nd Alloys Atomic percent	$\Delta\gamma_2(a)$	$\Delta\beta_2(a)$	$\Delta\gamma_2(b)$
1st Si		4.818	0.0191	467	1.08	0.029	−0.0009	0.025	2.06	0.111	−0.0023	0.092
2nd Si		4.812	0.0197	462		0.025	−0.0010	0.014		0.088	−0.0017	0.082
Al	III	4.815	0.0197	462	1.04	0.066	−0.0009	0.058	2.13	0.134	0.0003	0.141
1st Ni		4.800	0.0209	453	1.00	0.098	0.0007	0.104	3.53	0.483	0.0022	0.506
2nd Ni		4.824	0.0189	468		0.103	0.0000	0.104		0.497	−0.0002	0.500
Co		4.818	0.0184	472	0.89	−0.017	−0.0007	−0.025	3.71	−0.076	−0.0025	−0.104
1st Nb		4.782	0.0194	465	0.50	0.122	0.0016	0.123	1.13	0.271	0.0033	0.294
2nd Nb		4.788	0.0210	453		0.139	0.0025	0.138		0.290	−0.0000	0.301
1st W		4.830	0.0181	475	0.31	−0.046	0.0006	−0.044	0.62	−0.077	0.0005	−0.072
2nd W	II	4.826	0.0189	468		−0.044	0.0010	−0.041		−0.076	−0.0001	−0.071
3rd Mo		4.797	0.0198	461	1.16	−0.035	0.0002	−0.043	2.06	−0.088	0.0010	−0.077
1st Mo		4.809	0.0185	472		−0.038	0.0004	−0.035		−0.079	0.0008	−0.070
2nd Mo		4.815	0.0172	483		−0.050	0.0019	−0.036		−0.104	0.0026	−0.079
1st Cr		4.776	0.0217	448	0.46–0.53	−0.051	−0.0004	−0.055	0.88–1.00	−0.102	0.0002	−0.096
2nd Cr		4.797	0.0213	450		−0.034	−0.0024	−0.049		−0.096	0.0002	−0.091
1st V		4.767	0.0266	418	1.10	−0.106	−0.0016	−0.117	2.19–2.29	−0.217	−0.0023	−0.236
2nd V		4.728	0.0254	425		−0.114	−0.0002	−0.112		−0.216	−0.0019	−0.226
1st Mn	I	4.772	0.0231	438	1.14	0.114	−0.0024	0.099	2.21–2.25	0.231	−0.0015	0.225
2nd Mn		4.771	0.0227	441		0.119	−0.0021	0.103		0.245	−0.0030	0.225
1st Ti		4.799	0.0212	451	1.16	−0.067	0.0008	−0.059	2.32–2.36	−0.114	0.0008	−0.105
2nd Ti		4.776	0.0243	431		−0.042	−0.0026	−0.061		−0.096	−0.0016	−0.103
3rd Ti		4.807	0.0201	459		−0.069	0.0005	−0.062		−0.115	0.0004	−0.108

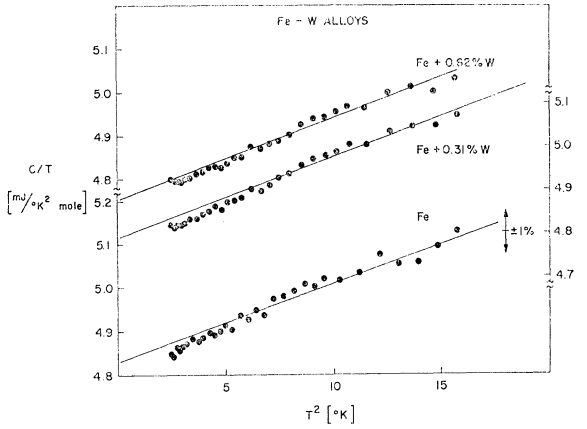

FIG. 5. Specific heat of Fe(W) alloys.

After these results the second manometer was added and the specific heat of silver-gold alloys was redetermined. Then the "magnetic" solutes were investigated using Fe(Co) and Fe(Ni) alloys. Finally nontransition elements were studied using Fe(Al) and Fe(Si) alloys. The absolute values from the later investigations (Group III) are taken to be more correct than those of the earlier investigations.

Because much data has been recently published concerning the specific heat of silver and also because there is some recent good data on Fe, we will discuss first the comparison of our results on the pure elements with previous work. We do this not because this paper is concerned with interpretation of absolute values, but for the purpose of establishing creditability. From an analysis of our data for Ag from 2 to 4°K in terms of Eq. (6) and the expression

$$\Theta_D = (1943/\beta)^{1/3}, \tag{7}$$

we may compare our results with the results of recent investigations; see Table I.

The maximum differences are at 4.2°K. There the

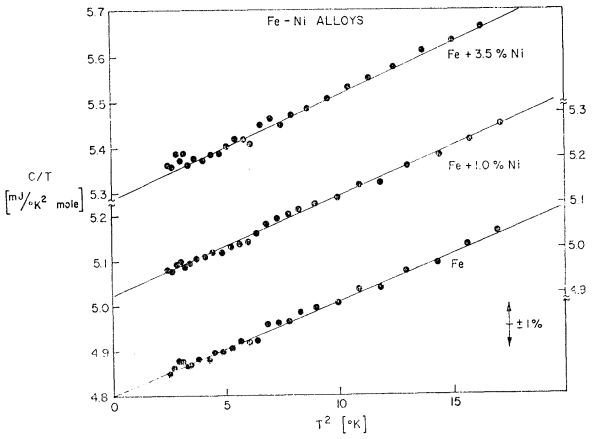

FIG. 6. Specific heat of Fe(Ni) alloys.

TABLE III. Comparison of results for iron.

Experimenters	γ[a]	Θ_D[a]
Our work (Group III)	4.81	463
Our work (Group II)	4.80	468
Our work (Group I)	4.77	440
Dixon, Hoare, Holden, and Moody[b]	4.78	464

[a] These values are for best fits to Eq. (6). Dixon *et al.* discuss corrections for contributions from spin waves.
[b] See Ref. 16.

data divide into two groups with our data, that of Green and Culbert[15] and that of Green and Valladares[6] lying almost a percent above the data of Dixon *et al.*,[16] the extrapolation of the data of Filby and Martin,[17] and the recalculated data of Corak *et al.*[18] As it is in this region that the carbon resistance thermometers are least sensitive and begin to deviate from Eq. (1), these differences are not surprising. A comparison of our results with the most recent data of Green and Valladares is seen in Fig. 4.

The specific heat of iron is measured in each of our many experiments with the Fe alloys. With modifications of apparatus we have found systematic differences in the Fe results. The most significant variations concern thermometry, or more particularly, the measurement of vapor pressure. Table II summarizes our data on Fe. The increase in γ with time we would assert is due to improved accuracy in the measurement of vapor pressure after we became aware of the difficulties with establishing the zero of pressure. If we compare our results for C/T of Fe with those of Dixon *et al.*, we find that, as in the case of Ag, our most recent results are greater by about 1%; see Table III.

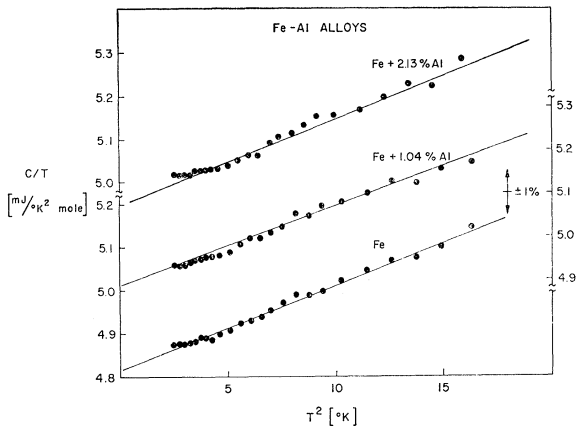

FIG. 7. Specific heat of Fe(Al) alloys.

[15] B. A. Green, Jr., and H. V. Culbert, Phys. Rev. **137**, A1168 (1965).
[16] M. Dixon, F. E. Hoare, T. M. Holden, and D. E. Moody, Proc. Roy. Soc. (London) **A285**, 561 (1965).
[17] J. D. Filby and D. L. Martin, Can. J. Phys. **40**, 791 (1962).
[18] W. S. Corak, M. P. Garfunkel, C. B. Satterthwaite, and A. Wexler, Phys. Rev. **98**, 1699 (1955).

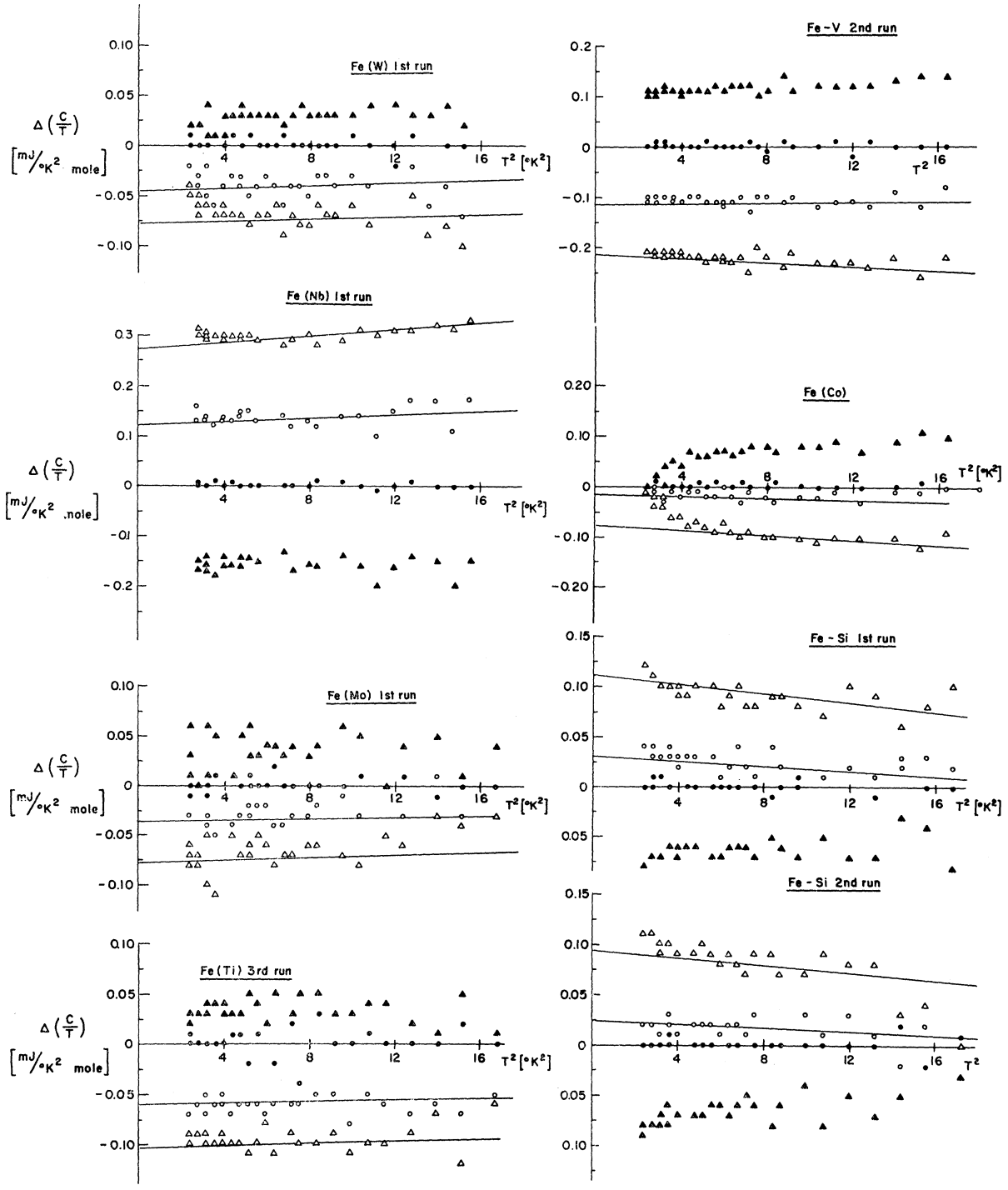

FIG. 8. Representative examples of specific-heat differences of Fe alloys: ●, differences of individual Fe points from a 5 point running average of the data points; ○, differences of alloy 1 and Fe point by point after small correction for temperature differences; △, same difference for alloy 2 and Fe; △, same difference for alloy 1 and alloy 2. Lines apparently drawn through data points are actually drawn from values of $\Delta\gamma_1(a)$, $\Delta\beta_1(a)$, $\Delta\gamma_2(a)$, and $\Delta\beta_2(a)$ of Table II.

In treating the Fe data we assume that the changes with alloy content can be represented by changes in the coefficients γ and β of Eq. (6). Dixon *et al.* have discussed possible magnetic contributions to the specific heat. They are very small, particularly above 2°K, where we work. In addition, because the Curie temperatures

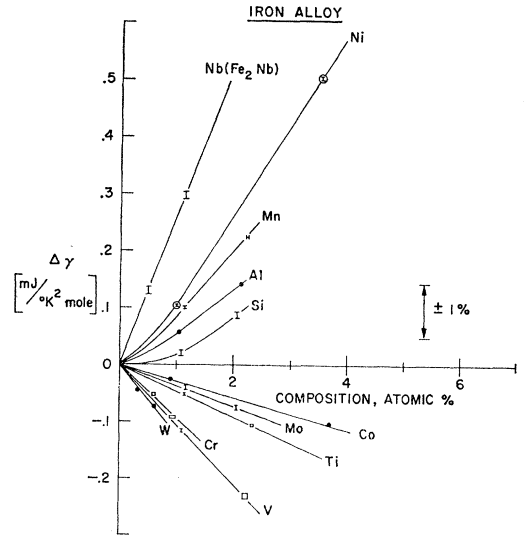

FIG. 9. Variation of γ with concentration for dilute alloys of Fe.

are so high and change only slowly with solute concentrations, it seems reasonable to ignore any changes in the small magnetic contributions when analyzing our data.

The data for the alloys were handled in two different manners. The first was a straightforward least-squares fit to Eq. (6) for each sample in the temperature range 2 to 4°K to obtain γ and β for Fe and the two alloys measured simultaneously. The fits for Fe-W, Fe-Ni and Fe-Al alloys are shown in Figs. 5, 6, and 7. The differences of the values $\gamma_i-\gamma_{Fe}\equiv\Delta\gamma_i(a)$ and $\beta_i-\beta_{Fe}\equiv\Delta\beta_i(a)$, where i stands for alloy 1 or 2, are tabulated in Table II.

The second method requires a little more explanation. We wish to make a point-by-point comparison of the specific heats in each run. As the three measurements are not at precisely the same temperatures, we must correct for these temperature differences before comparing the specific heats from three simultaneous measurements. We proceed as follows. Let T_0 by the mean temperature of a particular evaluation of the specific heat of the iron sample. We take 5 points, namely the data for T_0 and two points above and two points below T_0, and find values of γ and β, namely, γ_0 and β_0, which give a best fit for the five points. We then find $\langle(C_0/T_0)\rangle_{av}=\gamma_0+\beta_0T_0^2$. The difference between (C_0/T_0) observed and $\langle(C_0/T_0)\rangle_{av}$ is plotted in Fig. 8 with the symbol ●. We carry out a similar procedure to find γ_1, and β_1 and γ_2 and β_2 as the local best fit for any alloy samples 1 and 2. We calculate a temperature-shifted value of C/T for alloy sample one for the temperature T_0, which we call $(C_1/T_1)_0$, according to $(C_1/T_1)_0=(C_1/T_1)_1+\beta(T_0^2-T_1^2)$, where $(C_1/T_1)_1$ is the measured value of C/T for alloy sample 1 at a mean temperature T_1. We do the same for sample 2. We then calculate $(C_1/T_1)_0-(C_0/T_0)_0$ which are plotted as ○, $(C_2/T_2)_0-(C_0/T_0)_0$ which are plotted as △, and $(C_2/T_2)_0-(C_1/T_1)_0$ which are plotted as ▲. In other words, the base line in Fig. 8 is the running average of 5 points for the Fe sample; the ● are the differences of the individual Fe points from the base line. The ○, △, ▲ are direct differences in measured values after shifting the alloy sample points to correct for the slight differences in sample temperatures. Note that the data extend outside our range of thermometer calibration without any disastrous consequences. The lines apparently drawn through the points are actually the least-squares fits of all the data between 2 and 4°K, namely from the values $\Delta\gamma_1(a)$ and $\Delta\beta_1(a)$, $\Delta\gamma_2(a)$, and $\Delta\beta_2(a)$ of Table II. The two methods of treating the data are in good agreement. The next step is to use Fig. 8 to determine the change in γ from the point-by-point subtraction of the individual data points. These graphs illustrate the difficulty in determining the changes in β with confidence. The freedom to choose $\Delta\beta$ affects the choice of $\Delta\gamma$. Table II contains the values labeled $\Delta\gamma_1(b)$ and $\Delta\gamma_2(b)$ which are averages of the $\Delta(C/T)$ for all the points of each sample (except for the Co alloys where only the data above 2.5°K were averaged). That is, $\Delta\gamma_1(b)$ and $\Delta\gamma_2(b)$ are the changes in γ from Fig. 8 calculated as if there were no changes in β. If we compare the several runs on the same samples, we find that the variation in the $\Delta\gamma(b)$'s is less than that of the variation in the $\Delta\gamma(a)$'s. This is because of the uncertainties arising from the β degree of freedom in the fit to obtain the $\Delta\gamma(a)$'s.

We desired to calculate $(1/\beta)(d\beta/dc)$ from the elastic constants, but could not find values for single-crystal elastic constants of these alloys. We sought to estimate $(1/\beta)(d\beta/dc)$ from measurements of Young's-modulus changes for these polycrystalline alloys, but found that the sensitivity of Young's modulus to texture (statistically preferred orientations) and the sensitivity of texture to composition made this approach of no value. Therefore, we have presented the data in a form in which one can in the future correct for the changes in β with concentration.

Figure 9 summarizes our results showing $\Delta\gamma$ as a function of concentration. The data on the Fe-Nb system are for two-phase alloys with a solubility limit of 0.1% Nb in the Fe matrix. It does not appear reasonable to use these data to extract the specific heat of Fe (0.001 Nb) as one could in principle if the data were sufficiently accurate. One can extract an estimate of γ for Fe_2Nb of 9.5±0.5 mJ/mole/deg², that is, about twice that of iron.

Through the data for W, V, Cr, Ti, Mo, and Co, within experimental uncertainties, one can pass a straight line from the origin to obtain values for $d\gamma/dc$. For Ni, Mn, Al, and Si, however, the existence of a nonlinear variation with concentration appears to be outside the experimental scatter of the data. We cannot think of a systematic error which would affect only those samples with positive $d\gamma/dc$, except for the fact that three of these were the last samples measured.

TABLE IV. Concentration dependence of γ for dilute iron alloys.

	Al	Si	Mn	Ni
$(1/\gamma)(d\gamma/dc)_{av}$	1.2	0.6	2.0	2.6
	Ti	V	Cr	Co
$(1/\gamma)(d\gamma/dc)$	−1.0	−2.2	−2.0	−0.6
	Cr	Mo	W	
$(1/\gamma)(d\gamma/dc)$	−2.0	−0.8	−2.4	

Faced with a nonlinear behavior and only three data points, one cannot proceed further without assuming something about that nonlinear behavior, e.g., that it is a linear-plus-quadratic dependence. In Table IV we quote average values of $(1/\gamma)d\gamma/dc$ for these alloys. We are investigating with additional alloys the details of this nonlinear dependence of γ on composition for the Fe(Si) alloys.

The comparison of our data for Ag(Au) with those of Green and Valladares for more concentrated alloys is shown in Fig. 10. The big effect on alloying is the decrease in Θ_D arising from the heavy Au atoms. Though we disagree in the value of Θ_D for Ag by 0.2%, our values of $d\Theta_D/dc$ are indistinguishable from theirs. On the basis of our own results we would have quoted that $(1/\gamma)d\gamma/dc=0\pm1$. Green and Valladares find $(1/\gamma)d\gamma/dc=-0.3$.

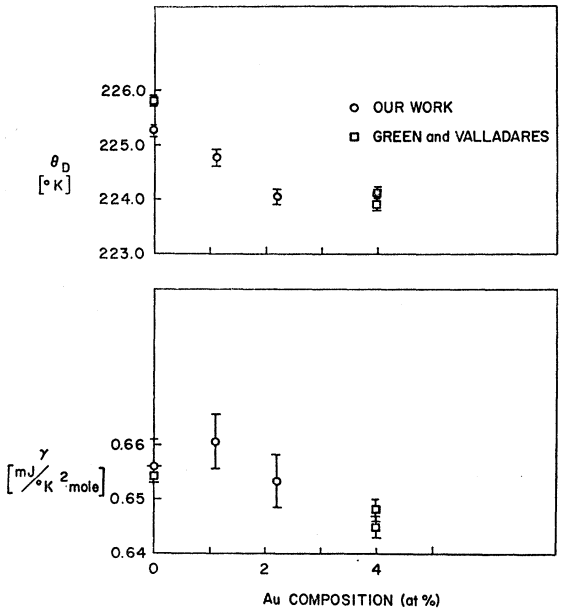

FIG. 10. Comparison of our work and that of Green and Valladares (Ref. 6) for the variation of γ and Θ_D with concentration for Ag(Au) alloys.

V. DISCUSSION

Brailsford[19] has provided a formulation of the dilute-alloy specific-heat problem. Alloys are considered dilute as long as the terms linear in concentration c are sufficient to describe the concentration dependence of the specific heat. Attention is focused on the shift of electronic energy levels $\epsilon(k)$ corresponding to wave vectors k, there being as many states as there are k vectors in a Brillouin zone. For a perturbation $V(r)$ there will be a change in energy of each of these states such that $\epsilon_A(k)=\epsilon_0(k)+\Delta(k,\epsilon_k)$. The total number of states below an energy ϵ in the pure metal $Z_0(\epsilon)$ will differ from that in the alloy $Z_A(\epsilon)$ by an amount which depends upon the energy shifts

$$Z_A(\epsilon)=Z_0(\epsilon)-N_0(\epsilon)\bar{\Delta}(\epsilon), \tag{8}$$

where

$$\bar{\Delta}(\epsilon)\equiv\frac{1}{4\pi^3N_0(\epsilon)}\int_{\epsilon_k=\epsilon}\frac{dS}{|\nabla\epsilon_k|}\Delta(k,\epsilon_k) \tag{9}$$

is the average energy shift for energy ϵ. From the definition of $Z(\epsilon)$, the density of states $N(\epsilon)\equiv dZ(\epsilon)/d\epsilon$, hence

$$N_A(\epsilon)=N_0(\epsilon)-(d/d\epsilon)\{N_0(\epsilon)\bar{\Delta}(\epsilon)\}. \tag{10}$$

Denoting the Fermi energy in the alloy by η_A and in the pure metal by η_0, one can write

$$Z_A(\eta_A)=Z_0(\eta_0)+N_0(\eta_0)\{\eta_A-\eta_0-\bar{\Delta}(\eta_0)\} \tag{11}$$

and

$$N_A(\eta_A)=N_0(\eta_0)+\frac{dN_0(\eta_0)}{d\eta_0}\times\{\eta_A-\eta_0-\Delta(\eta_0)\}-N_0(\eta_0)\frac{d\bar{\Delta}(\eta_0)}{d\eta_0}. \tag{12}$$

From these one obtains for the change in density of states on alloying

$$\delta N=N_A(\eta_A)-N_0(\eta_0)=\frac{1}{N_0(\eta_0)}\frac{dN_0(\eta_0)}{d\eta_0}\times\{Z_A(\eta_A)-Z_0(\eta_0)\}-N_0(\eta_0)\frac{d\bar{\Delta}(\eta_0)}{d\eta_0}. \tag{13}$$

As $Z_A(\eta_A)-Z_0(\eta_0)$ is the total number of electrons added upon alloying, the first term on the right is the contribution to the density of states from adding electrons without changing the band shape. This is the rigid-band term. The second term is descriptive of the way $N(\epsilon)$ is altered by the presence of the solutes. A constant value of $\bar{\Delta}(\epsilon)$ is just a shift of the energy origin for the whole $N(\epsilon)$ curve and does not change γ. It is the accumulation or depletion of states in the immediate vicinity of the Fermi energy which is of importance. For example, a solute which increases the energy of states which lie below the Fermi surface while decreasing that of states which lie above the Fermi surface increases γ. The results for pseudo-copper alloys or for Ag(Au) alloys may be at variance with expectations from considering only the rigid-band term, but when one considers the second term it becomes more difficult to draw conclusions. One needs a detailed calculation of the

[19] A. D. Brailsford, Proc. Roy. Soc. (London) **A292**, 433 (1966).

virtual scattering of the electrons by the solute potential in order to proceed. As the matrix elements used to calculate the energy shifts would also come into a calculation of resistivity, one might hope to obtain an experimental hold on the second term through studies of resistivity. But Brailsford has pointed out that detailed correlation between these effects is not to be expected. In this connection we note that Au additions increase the residual resistivity of Ag at the same rate at which Zn additions increase the residual resistivity of Cu, namely 0.3 $\mu\Omega$ cm/at.%.

In applying Brailsford's formalism to Fe and its dilute alloys, we must bear in mind the fact that in a ferromagnetic material the density of states for electrons of spin up and spin down are not likely to be the same and that in general the density of states for either one will not be completely negligible with respect to that of the other. Added electrons may go into each of the two bands in unequal numbers. The energy shifts, which depend upon scattering matrix elements, will be different for spin-up and spin-down electrons even though they have the same momentum. Thus, we rewrite Eq. (13) twice, once with superscripts $\uparrow$ added to N, Z, and Δ, and once with a superscript $\downarrow$. We note that

$$Z_A\uparrow(\eta_A)+Z_A\downarrow(\eta_A)-Z_0\uparrow(\eta_0)-Z_0\downarrow(\eta_0)=n\nu c, \quad (14)$$

where n is total number of atoms and ν the relative valence of the solute, and that

$$Z_A\uparrow(\eta_A)-Z_0\uparrow(\eta_0)-Z_A\downarrow(\eta_A)+Z_0\downarrow(\eta_0)=n\mu c, \quad (15)$$

where μ is the relative magnetization of the solute in Bohr magnetons. We find for the change in density of states

$$\delta N=\frac{d}{d\eta_0}[\ln N\uparrow(\eta_A)N\downarrow(\eta_0)]n\nu c/2 + \frac{d}{d\eta_0}\left[\ln\frac{N\uparrow(\eta_0)}{N\downarrow(\eta_0)}\right]n\mu c/2 - N\uparrow(\eta_0)\frac{d\Delta\uparrow(\eta_0)}{d\eta_0}-N\downarrow(\eta_0)\frac{d\Delta\downarrow(\eta_0)}{d\eta_0}. \quad (16)$$

The first two terms are the rigid-band terms. If $\mu=0$, electrons enter the two bands equally. If $\mu=\nu$, the electrons enter the band of spin up only. And if $\mu=-\nu$, the electrons enter the band of spin down only. Under certain assumptions one could obtain μ from spontaneous magnetization measurements. However, the lack of regularities in Table IV dooms to failure attempts to fit the specific-heat results using only the rigid-band terms. We have concluded from such attempts that the energy shift terms must be more important than the rigid-band terms. As one needs detailed models to discuss these terms, we do not pursue the analysis further.

We would call attention to one correlation. Fe(Mn) alloys and Fe(Ni) alloys are similar with respect to their phase diagrams. Both systems have an open γ loop with the α-γ transition temperature dropping rapidly with increasing solute concentration. Both systems have decreasing Curie temperatures with increasing solute concentrations. Neither of these features is found for Fe(Ti), Fe(V), Fe(Cr), or Fe(Co). One might try to explain these differences in phase diagram in terms of the rapidly increasing γ^* which is observed for Mn and Ni solutes and not for the other transition metal solutes. Yet the effect is the "wrong way." For the greater γ the more negative is the electronic contribution to the free energy and this would tend to make the low-temperature bcc magnetic phase more stable. Why the behavior should be the same for Mn and Ni solutes seems to be a mystery. One notes further that both Al and Si decrease the Curie temperature while increasing γ^*.

ACKNOWLEDGMENTS

The authors wish to express their thanks to Dr. H. Sato and Dr. A. D. Brailsford for valuable discussions of the dilute-alloy problem and for criticisms of the manuscript. Advice on experimental techniques has been obtained from Dr. G. L. Guthrie, Dr. J. E. Zimmerman, Professor F. E. Hoare, and Dr. N. Phillips. In the early stages of this work we benefited from the experimental assistance of Dr. J. Skalyo and R. A. Kane.